Solid State Communications 151 (2011) 1420–1423

Contents lists available at SciVerse ScienceDirect

Solid State Communications

journal homepage: www.elsevier.com/locate/ssc

Barrier height inhomogeneities in InN/GaN heterostructure based Schottky junctions

Basanta Roul [a,b], Thirumaleshwara N. Bhat [a], Mahesh Kumar [a,b], Mohana K. Rajpalke [a], Neeraj Sinha [c], A.T. Kalghatgi [b], S.B. Krupanidhi [a,*]

[a] Materials Research Centre, Indian Institute of Science, Bangalore-560012, India
[b] Central Research Laboratory, Bharat Electronics, Bangalore-560013, India
[c] Office of the Principal Scientific Advisor, Government of India, New Delhi-110011, India

ARTICLE INFO

Article history:
Received 8 March 2011
Received in revised form
8 June 2011
Accepted 6 July 2011
by R. Phillips
Available online 14 July 2011

Keywords:
A. Heterostructures
C. Schottky junctions
D. Thermionic emission

ABSTRACT

The electrical transport properties of InN/GaN heterostructure based Schottky junctions were studied over a wide temperature range of 200–500 K. The barrier height and the ideality factor were calculated from current–voltage (I–V) characteristics based on thermionic emission (TE), and found to be temperature dependent. The barrier height was found to increase and the ideality factor to decrease with increasing temperature. The observed temperature dependence of the barrier height indicates that the Schottky barrier height is inhomogeneous in nature at the heterostructure interface. Such inhomogeneous behavior was modeled by assuming the existence of a Gaussian distribution of barrier heights at the heterostructure interface.

1. Introduction

In recent years, III nitride materials have attracted the attention of the semiconductor research community because of their applications in light emitting diodes (LEDs), laser diodes, high efficiency solar cells and high frequency electronic devices [1–3]. The properties of InN such as the narrow band gap [4], the possibility of generation of THz emission [5] and superior electron transport properties [6] are very promising for numerous applications of this material. However, the high densities of different defects like edge, screw and mixed dislocations due to the high lattice mismatch of InN with other nitrides and high equilibrium pressure of nitrogen restrict the growth of InN epilayers and heterostructures with reasonable quality [7]. Due to the enormous effort put into improving the quality of InN epitaxial layers, heterostructure based devices have taken on much importance in semiconductor research communities. The interfaces of the heterostructure are important parts in the electronic and optoelectronic devices. One of the most interesting features of the interface is its Schottky barrier height (SBH), which is a measure of the mismatch of the energy levels for the majority carriers across the interface. The performances of the heterostructure based devices are strongly dependent on the homogeneity of the interfaces. In this work, we fabricated InN/GaN Schottky junctions and extensively studied the temperature dependent electrical transport behavior in order to evaluate the barrier height and ideality factor. We have found that the barrier height and the ideality factor were temperature dependent. The observed temperature dependence of the barrier height indicates that the Schottky barrier height is inhomogeneous in nature at the heterostructure interface. The inhomogeneous behavior was modeled by assuming the existence of a Gaussian distribution of barrier heights at the heterostructure interface.

2. Experimental

InN thin film of thickness around 300 nm was grown on 4 μm GaN/Al_2O_3 (0001) templates using an Omicron nanotechnology plasma assisted molecular beam epitaxy (PAMBE) system. The GaN template was degreased using acetone and propan-2-ol, etched using an HF:H_2O (1:10) solution and rinsed with deionized water before loading into the MBE chamber. The film was grown by using a two-step process: growth of a low temperature (400 °C) InN buffer layer of thickness 20 nm followed by the growth of an InN epilayer of thickness 280 nm at high temperature (500 °C). During the growth, the nitrogen pressure was kept at 2.8×10^{-5} mbar, corresponding to a nitrogen flow rate of 0.5 sccm, and the forward

* Corresponding author. Tel.: +91 80 2360 1330; fax: +91 80 2360 7316.
E-mail address: sbk@mrc.iisc.ernet.in (S.B. Krupanidhi).

0038-1098/$ – see front matter © 2011 Elsevier Ltd. All rights reserved.
doi:10.1016/j.ssc.2011.07.008

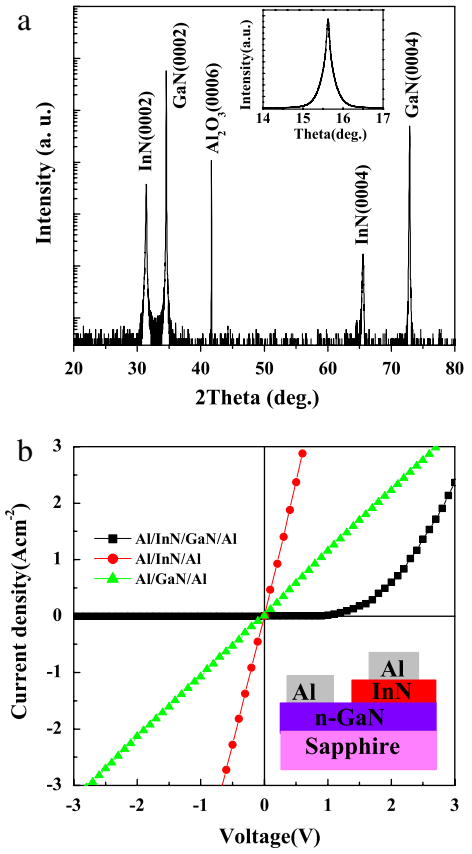

Fig. 1. (Color online) (a) 2θ–ω HRXRD scanning curve of InN film grown on a GaN template. The inset shows the XRC of the (0002) InN reflection. (b) Room temperature J–V measurement of the device. The inset shows the schematic of the device structure.

RF power of the plasma source was fixed at 350 W. Photolithography was carried out on the sample to define the junction area. Reactive ion etching (RIE, Anelva) was carried out on the InN film until the GaN layer was exposed for ohmic contact. Then the circular ohmic contacts were made on InN as well as on GaN layers by thermally depositing Al (thickness ∼200 nm) metal; this was followed by a thermal annealing at 200 °C for 20 min. The structural characterization of the film was carried out by means of high resolution X-ray diffraction (HRXRD) measurements using a double-crystal four-circle diffractometer (Bruker-D8 DISCOVER). The I–V measurements were performed by taking contacts from two Al metals deposited on InN and GaN layers. The I–V measurements were carried out by using a computer interfaced Keithley-236 source meter system in the temperature range of 200–500 K, in steps of 50 K in dark conditions.

3. Results and discussion

Fig. 1(a) shows a 2θ–ω HRXRD scan of InN film grown on a GaN/Al_2O_3 (0001) template. The peaks at $2\theta = 31.3°$ and 65.5° are assigned to the (0002) and (0004) planes of the InN film respectively. The peaks at $2\theta = 34.56°$ and 72.81° correspond to the (0002) and (0004) planes of the GaN film respectively. The structural quality of the InN film was evaluated from the full width at half-maximum (FWHM) of the X-ray rocking curve (XRC) of the (0002) InN reflection which is shown in the inset of Fig. 1(a). The XRC FWHM of the (0002) InN reflection was found to be 450 arcsec, which indicates that the InN film is highly crystalline in nature. Even though this value is comparable to the reported value [8], there could be a several defects like edge and screw dislocations

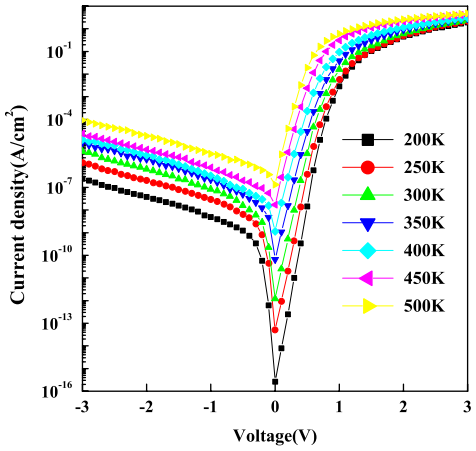

Fig. 2. (Color online) The forward J–V characteristics as a function of temperature for the InN/GaN Schottky junction.

present at the interface. The influence of defects on the SBH will be discussed in a later part. Fig. 1(b) shows the room temperature J–V measurement for the device. The schematic of the device structure is shown in the inset of Fig. 1(b). From room temperature J–V measurements, it is clear that the Al metal gives adequate ohmic contacts for both InN and GaN layers. The rectifying behavior of the J–V characteristic measurement suggests that the junction between InN and GaN exhibits a Schottky behavior. The forward and reverse current density–voltage (J–V) characteristics of the InN/GaN heterostructure in the temperature range of 200–500 K are shown in Fig. 2. The values of the SBH (ϕ_b) and the ideality factor (η) for the junction were calculated as functions of the measurement temperature by fitting a line in the linear region of the forward J–V curves using the thermionic emission (TE) model. From the TE theory, where $qV > 3kT$, the forward J–V characteristic of a Schottky diode is given by [9–11]

$$J = J_s \exp\left(\frac{qV}{\eta kT}\right) \tag{1}$$

where

$$J_s = A^* T^2 \exp\left(-\frac{\phi_b}{kT}\right). \tag{2}$$

Here, J_s is the saturation current density, T is the measurement temperature, $A*$ is the Richardson constant, k is the Boltzmann constant, q is the electron charge, ϕ_b is the Schottky barrier height and η is the ideality factor. The theoretical value of $A*$ was taken as 24 A cm^{-2} K^{-2} [9] for our calculations.

The values of ϕ_b and η at different temperatures were obtained from the linear region of the forward J–V characteristics by fitting Eq. (1). The variations of the barrier height and ideality factor with temperature are shown in Fig. 3. It is observed that there is a temperature dependent variation for both ϕ_b and η, i.e. ϕ_b increases and η decreases with increasing temperature. The temperature dependence of ϕ_b indicates that the SBH is inhomogeneous in nature. The inhomogeneous SBH may be due to various kinds of defects like edge and screw dislocations that could be present at the InN/GaN interface [12–14]. The values of ϕ_b and n obtained from J–V measurements at different temperatures are given in Table 1. Also, we have observed a linear relationship between ϕ_b and η, which is shown in the inset of Fig. 3.

For the evaluation of the barrier height, a Richardson plot of the saturation current can be utilized. Eq. (2) can be rewritten as

$$\ln\left(\frac{J_s}{T^2}\right) = \ln(A^*) - \frac{q\phi_b}{kT}. \tag{3}$$

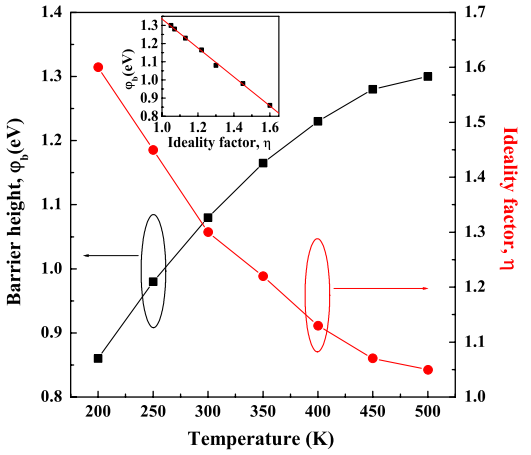

Fig. 3. (Color online) The temperature dependences of the barrier height and ideality factor obtained from forward bias J–V data using the thermionic emission model. The inset shows the plot of the barrier height versus the ideality factor at various temperatures.

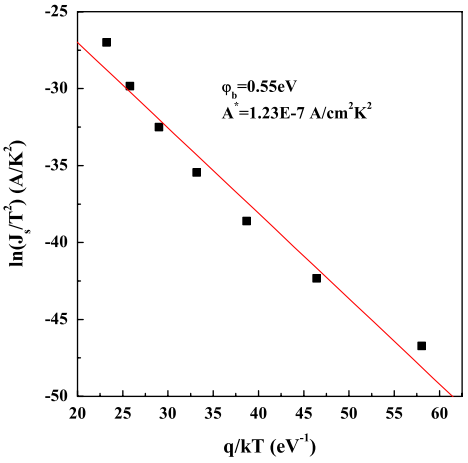

Fig. 4. (Color online) The conventional Richardson plot of $\ln(J_s/T^2)$ versus $1/kT$.

Table 1
The electrical parameters obtained from J–V measurements at different temperatures.

T (K)	J_s (A/cm^2)	η	ϕ_b (eV)
200	2.03×10^{-16}	1.6	0.86
250	2.61×10^{-14}	1.45	0.98
300	1.55×10^{-12}	1.3	1.08
350	4.93×10^{-11}	1.22	1.165
400	1.22×10^{-9}	1.13	1.23
450	2.24×10^{-8}	1.07	1.28
500	4.73×10^{-7}	1.05	1.3

The values of the saturation current density (J_s) were obtained at each temperature from the J–V data. The conventional Richardson plot of $\ln(J_s/T^2)$ versus $1/kT$ was obtained and is shown in Fig. 4. From the linear fit of the plot, the Richardson constant and the barrier height were calculated to be 1.23 $\times$ 10^{-7} A cm^{-2} K^{-2} and 0.55 eV respectively. The value of the Richardson constant obtained from the conventional Richardson plot is much lower than the theoretical value. Also, the value of the barrier height is less than the experimental value, suggesting the formation of an inhomogeneous barrier height at the interface.

The inhomogeneous nature of the SBH at the heterostructure interface has been modeled precisely by assuming a lateral distribution of the SBH with a Gaussian distribution [15–17]. Let us assume a Gaussian distribution of the barrier height in the

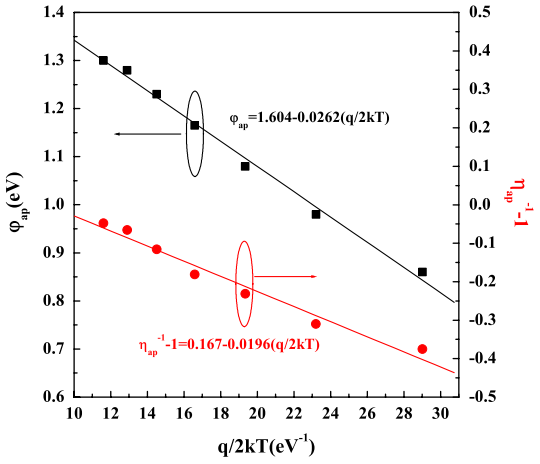

Fig. 5. (Color online) Plot of ϕ_{ap} versus $q/2kT$ and $(\eta_{ap}^{-1} - 1)$ versus $q/2kT$.

form

$$P(\phi_b) = \frac{1}{\sigma_s\sqrt{2\pi}} \exp\left[-\frac{(\phi_b - \overline{\phi_b})^2}{2\sigma_s^2}\right] \tag{4}$$

where $1/\sigma_s\sqrt{2\pi}$ is the normalization constant and $\overline{\phi_b}$ and σ_s are the mean and standard deviation of the barrier height respectively. The total current density at the forward bias V is given by

$$J(V) = \int_{-\infty}^{+\infty} J(\phi_b, V)P(\phi_b)\mathrm{d}\phi \tag{5}$$

where $J(\phi_b, V)$ is the current density at a bias voltage V for a barrier height of ϕ_b based on the TE model. Substituting Eqs. (1) and (4) into Eq. (5) and performing integration this becomes

$$J(V) = J_s \exp\left(\frac{qV}{\eta_{ap}kT}\right) \tag{6}$$

with

$$J_s = A^*T^2 \exp\left(-\frac{\phi_{ap}}{kT}\right) \tag{7}$$

where J_s is the saturation current density. The apparent barrier height (ϕ_{ap}) and apparent ideality factor (η_{ap}) are given by

$$\phi_{ap} = \overline{\phi_{b0}} - \frac{q\sigma_s^2}{2kT} \tag{8}$$

$$(\eta_{ap}^{-1} - 1) = \rho_2 - \frac{q\rho_3}{2kT} \tag{9}$$

where $\overline{\phi_{b0}}$ is the zero-bias mean barrier height and σ_s is the standard deviation, which are linearly bias dependent on Gaussian parameters, such as $\overline{\phi_b} = \overline{\phi_{b0}} + \rho_2$ V and $\sigma_s = \sigma_{so} + \rho_3$ V, where ρ_2 and ρ_3 are the voltage coefficients quantifying the voltage deformation of the barrier height distribution. According to Eq. (8), the plot of ϕ_{ap} versus $q/2kT$ should be a straight line whose intercept point is equal to the zero-bias mean barrier height ($\overline{\phi_{b0}}$) and the slope gives the standard deviation (σ_s), measuring the extent of the inhomogeneities present at the interface. Eqs. (1) and (6) are of the same form, so the fitting of Eq. (6) to the experimental J–V data gives the values of ϕ_{ap} and η_{ap}, respectively, which should obey Eqs. (8) and (9). Fig. 5 shows the plots of ϕ_{ap} versus $q/2kT$ and $(\eta_{ap}^{-1} - 1)$ versus $q/2kT$. The intercept and slope of ϕ_{ap} versus $q/2kT$ plot gives the values of $\overline{\phi_{b0}}$ and σ_s as 1.60 eV and 0.161 V respectively. On the other hand, the $(\eta_{ap}^{-1} - 1)$ versus $q/2kT$ plot should be a straight line whose intercept and slope give the values

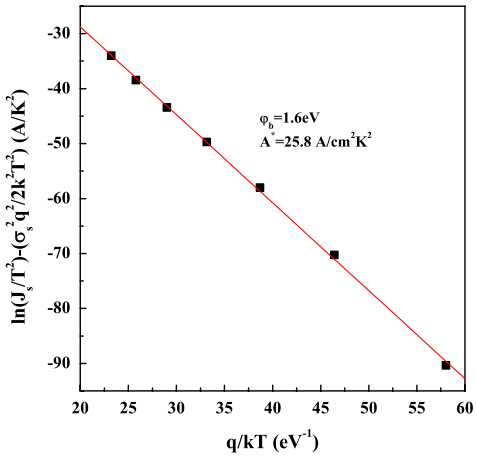

Fig. 6. (Color online) Modified Richardson plot of $\ln(J_s/T^2) - q^2\sigma_s^2/2k^2T^2$ versus q/kT.

of the voltage coefficients ρ_2 and ρ_3, respectively. The values of ρ_2 and ρ_3 were obtained as 0.167 V and 0.019 V respectively.

Considering the barrier height inhomogeneities, the conventional Richardson plot is modified by combining Eq. (2) with (7) as follows:

$$\ln\left(\frac{J_s}{T^2}\right) - \left(\frac{q^2\sigma_s^2}{2k^2T^2}\right) = \ln(A^*) - \frac{q\overline{\phi_{b0}}}{kT}. \tag{10}$$

According to Eq. (10), the modified plot $\ln(J_s/T^2) - q^2\sigma_s^2/2k^2T^2$ versus q/kT should give a straight line whose intercept point determines the value of $A*$, the slope giving the zero-bias mean barrier height ($\overline{\phi_{b0}}$). From the linear fit to the plot given in Fig. 6, the Richardson constant and the barrier height were calculated to be 25.8 A cm^{-2} K^{-2} and 1.6 eV respectively. The value of the Richardson constant obtained from the modified Richardson plot is very close to the theoretical value of 24 A cm^{-2} K^{-2}. Further, the values of $\overline{\phi_{b0}}$ obtained from Figs. 5 and 6 are in good agreement with each other. The higher value of the ideality factor (greater than unity) as estimated by using the TE model and the higher value of the barrier height as obtained from the modified Richardson plot suggest that the current transport may be dominated by thermionic field emission (TFE). The inhomogeneous behavior was modeled by assuming a Gaussian distribution of barrier heights that prevail at the heterostructure interface.

4. Conclusions

The electrical transport properties of InN/GaN heterostructure based Schottky junctions were studied over the wide temperature range of 200–500 K in steps of 50 K. The barrier height and the ideality factor were calculated from current–voltage (I–V) characteristics based on the thermionic emission (TE), found to be temperature dependent. The barrier height increased and the ideality factor decreased with increasing temperature. The observed temperature dependence of the barrier height indicates that the SBH is inhomogeneous in nature at the heterostructure interface. The inhomogeneous behavior was modeled by assuming the existence of a Gaussian distribution of barrier heights at the heterostructure interface.

References

[1] J.C. Lin, Y.K. Su, S.J. Chang, W.H. Lan, K.C. Huang, W.R. Chen, C.Y. Huang, W.C. Lai, W.J. Lin, Y.C. Cheng, Appl. Phys. Lett. 91 (2007) 173502.
[2] O. Jani, I. Ferguson, C. Honsberg, S. Kurtz, Appl. Phys. Lett. 91 (2007) 132117.
[3] C.J. Neufeld, N.G. Toledo, S.C. Cruz, M. Iza, S.P. DenBaars, U.K. Mishra, Appl. Phys. Lett. 93 (2008) 143502.
[4] V.M. Polyakov, F. Schwierz, Appl. Phys. Lett. 88 (2006) 032101.
[5] R. Ascazubi, I. Wilke, K. Denniston, H. Lu, W.J. Schaff, Appl. Phys. Lett. 84 (2004) 4810.
[6] V.W. Chin, T.L. Tansley, T. Osotchan, J. Appl. Phys. 75 (1994) 7365.
[7] Q. Guo, O. Kato, A. Yoshida, J. Appl. Phys. 73 (1993) 7969.
[8] K.A. Wang, T. Kosel, D. Jena, Phys. Stat. Sol. C 5 (2008) 1811.
[9] L. Wang, M.I. Nathan, T. Lim, M.A. Khan, Q. Chen, Appl. Phys. Lett. 68 (1996) 1267.
[10] H. Morkoç, Handbook of Nitride Semiconductors and Devices, Wiley-VCH, 2008.
[11] M. Shur, Physics of Semiconductor Devices, Prentice-Hall, Englewood Cliffs, NJ, 1990.
[12] K. Wang, C. Lian, N. Su, D. Jena, J. Timler, Appl. Phys. Lett. 91 (2007) 232117.
[13] A. Hattab, J.L. Perrossier, F. Meyer, M. Barthula, H.J. Osten, J. Griesche, Mater. Sci. Eng. B 89 (2002) 284.
[14] F.E. Cimilli, M. Saglam, A. Turut, Semicond. Sci. Technol. 22 (2007) 851.
[15] J.H. Werner, H.H. Güttler, J. Appl. Phys. 69 (1991) 1522.
[16] S. Acar, S. Karadeniz, N. Tugluoglu, A.B. Selcuk, M. Kasap, Appl. Surf. Sci. 233 (2004) 373.
[17] F.E. Jones, B.P. Wood, J.A. Myers, C. Daniels-Hafer, M.C. Lonergan, J. Appl. Phys. 86 (1999) 6431.